Aggregation and Alkylation of Enolates of 2-Phenyl-α-tetralone and 2,6-Diphenyl-α-tetralone[1]

Daniel Zerong Wang, Yeong-Joon Kim, and Andrew Streitwieser*
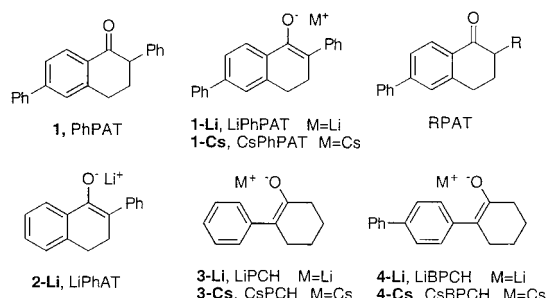
Contribution from the Department of Chemistry, University of California, Berkeley, California 94720-1460

Received March 20, 2000

Abstract: The cesium (**1-Cs**, CsPhPAT) and lithium (**1-Li**, LiPhPAT) enolates of 2,6-diphenyl-α-tetralone, **1**, and the lithium enolate (**2-Li**, LiPhAT) of 2-phenyl-α-tetralone, **2**, are present in dilute THF solution as monomers and dimers with $K_{1,2}$ = 1810 (**1-Cs**, CsPhPAT), 2650 (**1-Li**, LiPhPAT), and 1930 (**2-Li**, LiPhAT) M^{-1}. These values were obtained by singular value decomposition analysis of the UV spectra and by the dependence of ion pair pK's with concentration. On the ion pair pK scales previously defined, the monomers have pK = 17.80 (**1-Cs**, CsPhPAT) and 11.14 (**1-Li**, LiPhPAT). The monomers are much faster than dimers in alkylation reactions; reaction products from alkyl halides are those of C-alkylation, but **1-Cs** (CsPhPAT) with methyl sulfonates gives large amounts of O-alkylation. Comparison with previous results shows that the reactivity of cesium enolates parallels their basicity but that lithium enolates show no correlation between ion pair pK and alkylation reactivity.

Introduction

Lithium enolates have long been known to be frequently aggregated in ethereal solvents.[2−8] We have recently reported the aggregation equilibrium constants in THF of several lithium and cesium enolates.[9−15] In the present paper these studies are extended to the lithium (LiPhPAT, **1-Li**) and cesium (CsPhPAT, **1-Cs**) enolates of 2,6-diphenyl-α-tetralone. The ketone, PhPAT, **1**, is related to the *p*-phenylisobutyrophenone studied previously,[9,14] but the enolates are more conjugated. Deprotonation gives the conjugated enolates directly without the enolate isomer problem that complicated the study the enolates of α-phenyl- (MPCH) and α-*p*-biphenylylcyclohexanone (MBPCH).[7,8,15] Moreover, the tetralone ring system provides a rigid architecture in which the enolate double bond is constrained to conjugation with the benzene ring. The lithium enolate of α-tetralone has

1, PhPAT

1-Li, LiPhPAT M=Li
1-Cs, CsPhPAT M=Cs

RPAT

2-Li, LiPhAT

3-Li, LiPCH M=Li
3-Cs, CsPCH M=Cs

4-Li, LiBPCH M=Li
4-Cs, CsBPCH M=Cs

been shown to be predominantly a monomer−tetramer equilibrium in THF by NMR techniques, but with addition of a 2-isopropyl group the enolate is predominantly a dimer.[4] It was therefore important to determine the effect of a 2-phenyl substituent. Because of the extended conjugation in PhPAT enolate, the 6-phenyl substituent is not really necessary; it was included for comparison with a series of alkyl-substituted compounds, RPAT, that we plan to report on and in which the 6-phenyl substituent is necessary for study by UV spectroscopy. In this paper, however, we also include a more limited study of the lithium enolate of the parent system without the 6-phenyl group, LiPhAT, **2-Li**.

Results and Discussion

UV−Vis Spectra of Enolates. PhPAT, **1**, is a known compound and was prepared in low yield by a slight modification of the literature $S_{RN}1$ reaction.[16] Because the $S_{RN}1$ reaction proceeds in poor yield with α-tetralones and the product is difficult to separate from unreacted reactant, PhAT was prepared by cyclization of 2,4-diphenylbutanoic acid. The cesium enolate of PhPAT was generated by adding a THF solution of diphenylmethylcesium (CsDPM) to known amounts of the

(1) Carbon Acidity. 113.
(2) Horner, J. H.; Vera, M.; Grutzner, J. B. *J. Org. Chem.* **1986**, *51*, 4212−20.
(3) Jackman, L.; M.; Lange, B. C. *Tetrahedron* **1977**, *33*, 2737−2769.
(4) Jackman, L. M.; Bortiatynski, J. *Adv. Carbanion Chem.* **1992**, *1*, 45−87.
(5) Palmer, C. A.; Arnett, E. M. *J. Am. Chem. Soc.* **1990**, *112*, 7354−7360.
(6) Streitwieser, A.; Leung, S. S.-W.; Kim, Y.-J. *Org. Lett.* **1999**, *1*, 145−7.
(7) Streitwieser, A.; Wang, D. Z.-R. *J. Am. Chem. Soc.* **1999**, *121*, 6213−9.
(8) Wang, D. Z.-R.; Streitwieser, A. *Can. J. Chem.* **1999**, *77*, 654−8.
(9) Abbotto, A.; Streitwieser, A. *J. Am. Chem. Soc.* **1995**, *117*, 6358−9.
(10) Abu-Hasanayn, F.; Stratakis, M.; Streitwieser, A. *J. Org. Chem.* **1995**, *60*, 4688−9.
(11) Abbotto, A.; Leung, S. S.-W.; Streitwieser, A.; Kilway, K. V. *J. Am. Chem. Soc.* **1998**, *120*, 10807−13.
(12) Bauer, W.; Seebach, D. *Helv. Chim. Acta* **1984**, *67*, 1972−88.
(13) Ciula, J. C.; Streitwieser, A. *J. Org. Chem.* **1992**, *57*, 431−432; correction p 6686.
(14) Streitwieser, A.; Krom, J. A.; Kilway, K. A.; Abbotto, A. *J. Am. Chem. Soc.* **1998**, *120*, 10801−6.
(15) Streitwieser, A.; Wang, D. Z.; Stratakis, M. *J. Org. Chem.* **1999**, *64*, 4860−4.

(16) Scamehorn, R. G.; Hardacre, J. M.; Lukanich, J. M.; Sharpe, L. R. *J. Org. Chem.* **1984**, *49*, 4881.

ketone with biphenylyldiphenylmethane (BDPM) as an end point indicator. Known increments of THF were added, and the spectra were taken as a function of enolate concentration. The corresponding lithium enolate was generated by adding a solution of 9,9,10-trimethyl-9,10-dihydroanthracyllithium as base which also serves as its own end point indicator. Again, increments of THF were added to the UV cell and the spectra were taken. The resulting spectra were deconvoluted to remove any contribution of absorption from the indicator. The spectral data are detailed in Tables S1 and S2 (Supporting Information). For **1-Cs** (CsPhPAT) λ_{max} varies from 430.5 to 441.0 nm over the concentration range 1.0×10^{-3} to 1.3×10^{-5} M (Figure S1, Supporting Information), whereas for the lithium enolate **1-Li** (LiPhPAT) the maximum absorption wavelength was found in the range of 392.5−415.0 nm over the concentration range 9.0×10^{-4} to 8.5×10^{-6} M (see Figure S5, Supporting Information). This behavior has been observed for other enolates in which different aggregates have different λ_{max} and for which the extinction coefficients are approximately the same per enolate unit in the aggregates. The extinction coefficient at λ_{max} was found by a linear plot of the absorbance vs the formal concentration to give $\epsilon = 19366 \pm 62$ and 19820 ± 49 for CsPhPAT and LiPhPAT, respectively (Figures S4 and S8, Supporting Information). When these spectra are normalized to a common concentration, an isosbestic point appears at 441.0 nm for **1-Cs** (CsPhPAT) and 404.0 nm for **1-Li** (LiPhPAT) (Figures S2 and S6, respectively; Supporting Information). The isosbestic points show that only two concentration-dependent species are observable in each solution. These isosbestic wavelengths also provide better points for analysis and their extinction coefficients were determined: **1-Cs** (CsPhPAT), $\epsilon = 18639 \pm 62$; **1-Li** (LiPhPAT), $\epsilon = 19004 \pm 24$ (Figures S3 and S7, respectively, Supporting Information).

Similarly, spectral data were obtained for **2-Li** (LiPhAT) as detailed in Table S3 and Figures S9−S11 (Supporting Information); λ_{max} varies from 366 to 378 nm over the concentration range 1.3×10^{-3} to 5.7×10^{-5} M with an isosbestic point at 372 nm and an extinction coefficient of 16992 ± 60. The reduced conjugation with the absence of the 6-phenyl substituent results in a significant reduction of both λ_{max} and ϵ. The lithium enolate was prepared by treating a solution of the ketone with a slight excess of LiHMDS and diluting with known amounts of THF.

SVD Analysis. As in our previous studies, the method of singular value decomposition (SVD)[17] was applied to the spectral data. Consistent results were obtained only for the assumption of monomer−dimer mixtures. For **1-Cs** (CsPhPAT), the first three significant coefficients are $S_1 = 48.62$, $S_2 = 1.12$, and $S_3 = 0.14$, and for **1-Li** (LiPhPAT), $S_1 = 39.00$, $S_2 = 1.66$, and $S_3 = 0.089$. In both cases the small magnitude of the third significant coefficient indicates that any third component is negligible, in agreement with the observation of isosbestic points. From the SVD analysis the spectra of the monomer and dimer of **1-Cs** (CsPhPAT) and **1-Li** (LiPhPAT) are shown in Figure 1; λ_{max} values are **1-Cs** (CsPhPAT), monomer, 445.0 nm, dimer, 425.0 nm; and **1-Li** (LiPhPAT), 417.0 nm, dimer, 385.0 nm. As in previous cases, the dimer is at shorter wavelengths than the monomer.[7,8,11,14,15]

From these derived spectra the amounts of monomer and dimer were determined for each of the experimental spectra with results summarized in Tables S1 and S2 (Supporting
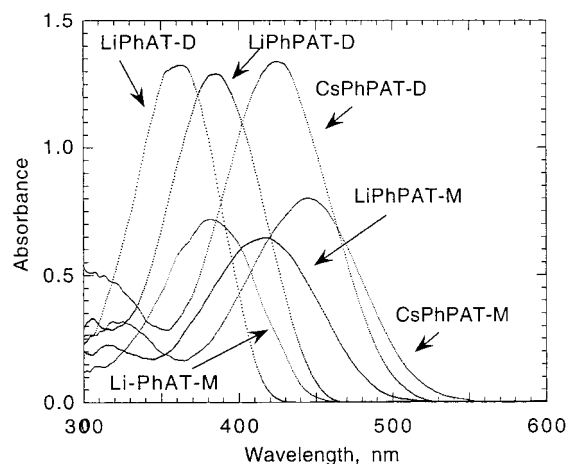
(17) Krom, J. A.; Petty, J. T.; Streitwieser, A. *J. Am. Chem. Soc.* **1993**, *115*, 8024−30.

Figure 1. The spectra of **2-Li** (LiPhAT), **1-Li** (LiPhPAT), and **1-Cs** (CsPhPAT) monomers and dimers from SVD analysis; λ_{max} are **1-Cs** (CsPhPAT), monomer, 445.0 nm, dimer, 425.0 nm; **1-Li** (LiPhPAT), 417.0 nm, dimer, 385.0 nm; **2-Li** (LiPhAT), monomer, 381.5 nm, dimer, 361.5 nm.

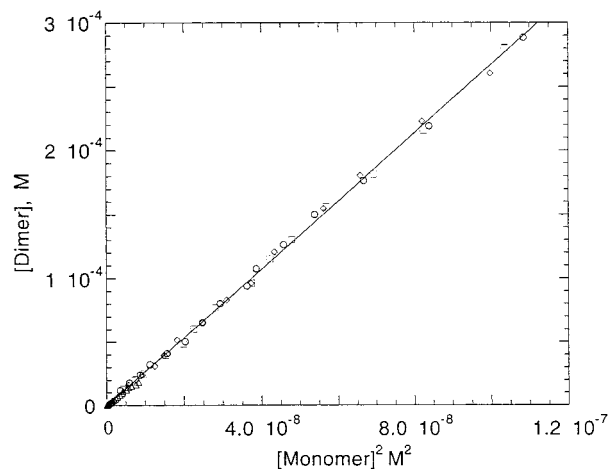**Figure 2.** Plot of [dimer] versus [monomer]^2 for **1-Li** (LiPhPAT). Line shown through the origin has slope $= 2673 \pm 9$, $R^2 = 0.999$.

Information). For the monomer−dimer equilibrium, eq 1, the corresponding equilibrium constant, $K_{1,2}$, is given by eq 2. For

$$2 \text{ monomer} \underset{}{\overset{K_{1,2}}{\rightleftharpoons}} \text{dimer} \tag{1}$$

$$K_{1,2} = \frac{[\text{dimer}]}{[\text{monomer}]^2} \tag{2}$$

1-Cs (CsPhPAT), four experiments in 1 mm UV cells give reproducible $K_{1,2}$ values, 1766 ± 6 M^{-1}, as shown in Figure S12 (Supporting Information). Similarly, for **1-Li** (LiPhPAT), four experiments give $K_{1,2} = 2673 \pm 9$ M^{-1}, as shown in Figure 2. The linearity of these plots also establishes that the aggregation equilibrium is between monomer and dimer. The more limited data for **2-Li** (LiPhAT) give a plot of comparable quality with $K_{1,2} = 1933 \pm 3$ M^{-1}, as shown in Figure S13 (Supporting Information). All three enolates show dimerization constants of comparable magnitude.

In past work we have learned that the *precision* of the SVD results is generally better than the *accuracy* and that a useful test for systematic errors is to compare the extrapolated values of λ_{max} for monomer and dimer from a plot of the experimental λ_{max} vs mole fraction of monomer with the values derived from SVD. Such plots are shown in Figures S14−S16 (Supporting

Information); the extrapolated values for **1-Cs** (CsPhPAT), M = 443 nm, D = 421 nm, for **1-Li** (LiPhPAT), M = 415 nm, D = 377 nm, and for **2-Li** (LiPhAT), M = 384 nm, D = 356 nm, are all in satisfactory agreement with the SVD values.

Proton Transfer Equilibria. Proton transfer equilibria between enolates and appropriate indicators provide a completely independent measure of aggregation constants. In such ion pair equilibria, eq 3, aggregation of the enolate $R^- M^+$ makes the observed proton transfer equilibrium constant, K_{ob}, concentration dependent. In eq 4, K_{ob} is given in terms of the formal enolate concentration denoted by braces, $\{R^-M^+\}$. This equilibrium constant is equivalent to the observed ΔpK difference between ketone and indicator; the observed pK is given by eq 5 and is also concentration dependent. As shown previously,[17] for a monomer–dimer equilibrium a plot of K_{ob} vs $\{R^-M^+\}/K_{ob}$ gives both K_o, the equilibrium acidity of the monomer relative to the indicator, and the aggregation equilibrium constant $K_{1,2}$ by eq 6.

$$\text{RH} + \text{In}^-\text{M}^+ \overset{K_0}{\rightleftharpoons} \text{R}^-\text{M}^+ + \text{InH} \tag{3}$$

$$K_{ob} = \frac{\{R^-M^+\}[\text{In-H}]}{[\text{RH}][\text{In}^-M^+]} \tag{4}$$

$$pK_{ob}(\text{RH}) = pK(\text{InH}) - \log K_{ob} \tag{5}$$

$$K_{ob} = K_0 + 2K_{1,2}K_0^2\{R^-M^+\}/K_{ob} \tag{6}$$

In these equations the subscript "ob" emphasizes that these experimental values are concentration dependent when R^-M^+ is aggregated, but will often be omitted when the context is clear.

Suitable indicators must satisfy several criteria: (a) the proton transfer equilibrium constant should not differ too much from unity, (b) the spectrum of the deprotonated indicator should differ significantly from that of the enolate, (c) the extinction coefficients of deprotonated indicator and enolate should permit measurement of both, and (d) the deprotonated indicator should be monomeric in the solution. On the basis of the these criteria, 9-biphenylylfluorene (BpFl, Cs salt: λ_{max} = 445.0 nm, pK = 17.72, ϵ_{max} = 29 400) and 9-phenylfluorene (PhFl, Cs salt: λ_{max} = 397.0 nm, pK = 18.15, ϵ_{max} = 24 000)[18] were chosen as indicators for **1-Cs** (CsPhPAT) and 1,3-diphenylindene (DPI, Li salt: λ_{max} = 450.0 nm, pK = 12.32, ϵ_{max} = 32 900)[19] was used as the indicator for **1-Li** (LiPhPAT). The indicator pK's are relative to assumed standards, the contact ion pair (CIP) cesium salt and solvent-separated ion pair (SSIP) lithium salt of fluorene assigned the DMSO value of 23.9 (per hydrogen).[20]

We note that we are generally careful to refer to these proton transfer equilibria in THF as "ion pair acidities" and to use the symbol "pK"; in particular, they are not pK_a's! Many so-called pK_a values have been assigned improperly in nonpolar solvents such as THF and CH_2Cl_2. pK_a refers to ionic dissociation to conjugate base and solvated protons; thus, the pK values in DMSO[20] are pK_a's because they refer back to measurements of $[H^+]$ in DMSO by glass electrode.[21,22] The ΔpK values from eq 5 can be converted to ΔpK_a values by use of the correspond-

(18) Streitwieser, A.; Ciula, J. C.; Krom, J. A.; Thiele, G. *J. Org. Chem.* **1991**, *56*, 1074−6.

(19) Streitwieser, A.; Wang, D. Z.; Stratakis, M.; Facchetti, A.; Gareyev, R.; Abbotto, A.; Krom, J. A.; Kilway, K. V. *Can. J. Chem.* **1998**, *76*, 765−9.

(20) Bordwell, F. G. *Acc. Chem. Res.* **1988**, *21*, 456−63.

(21) Kolthoff, I. M.; Reddy, T. B. *Inorg. Chem.* **1962**, *1*, 189.

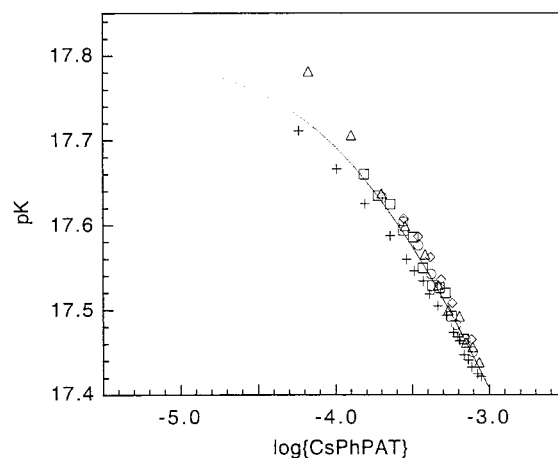(22) Ritchie, C. D.; Uschold, R. E. *J. Am. Chem. Soc.* **1967**, *89*, 1721−5.

Figure 3. Observed pK (Cs) for **1** (PhPAT). Small points show the calculated pK for $K_{1,2}$ = 1810 M^{-1} and pK_0 = 17.80. Squares, diamonds, and circles are observed pK vs BpFl as indicator (three series); triangles and pluses are observed pK vs PhFl as indicator (two series).
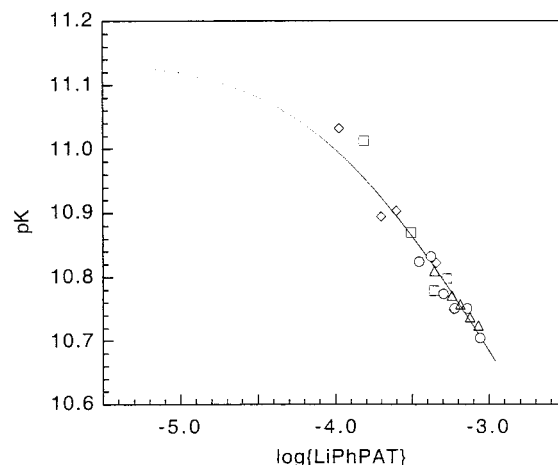

Figure 4. Plot of observed pK(Li) fot **1** (PhPAT) vs log{LiPhPAT}. Small points show the calculated pK for $K_{1,2}$ = 2650 M^{-1} and pK_0 = 11.14. Squares, diamonds, circles, and triangles are four series with DPI as indicator.

ing ion pair dissociation constants,[23,24] but without some known acid in THF, absolute pK_a values cannot be assigned. Only a few such values have been measured in THF and only for relatively strong acids.[25,26]

Several series of experiments were run by mixing known amounts of indicator and enolate, taking the spectrum and diluting incrementally with THF. The results are detailed in Tables S4−S6 (Supporting Information). The lithium equilibria were corrected for the small amount of dissociation of the LiIn to free ions in the dilute solutions used.[7] As expected, the observed pK's vary with concentration (Figures 3 (Cs) and 4 (Li)). The data were plotted according to eq 6 to give the results summarized in Figures 5 and 6. The two indicators with **1-Cs** (CsPhPAT) give pK_0 = 17.81, $K_{1,2}$ = 1875 M^{-1} and pK_0 = 17.79, $K_{1,2}$ = 1799 M^{-1}. The results agree well with each other and with the $K_{1,2}$ derived above from SVD. We adopt the average values as pK_0 = 17.80, $K_{1,2}$ = 1810 M^{-1}. The calculated

(23) Kaufman, M. J.; Gronert, S.; Streitwieser, A., Jr. *J. Am. Chem. Soc* **1988**, *110*, 2829−35.

(24) Antipin, I. S.; Gareyev, R. F.; Vedernikov, A. N.; Konovalov, A. I. *J. Phys. Org. Chem.* **1994**, *7*, 181−91.

(25) Coetzee, J. F.; Deshmukh, B. K.; Liao, C.-C. *Chem. Rev.* **1990**, *90*, 827−35.

(26) Deshmukh, B. K.; Siddiqui, S.; Coetzee, J. F. *J. Electrochem. Soc.* **1991**, *138*, 124−132.
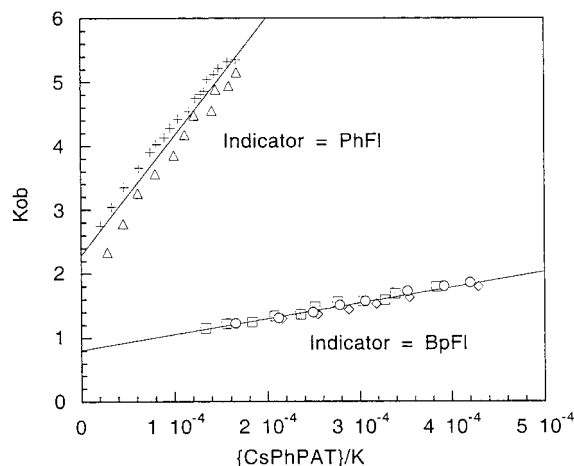
Figure 5. Plots of K_{ob} vs {CsPhPAT (**1-Cs**)}/K_{ob} for three runs with BpFl as indicator (line shown is $(0.805 \pm 0.03) + (2460 \pm 109)$-{CsPhPAT}/$K_0$; $R^2 = 0.957$) and two runs with PhFl as indicator (line shown is $(2.28 \pm 0.11) + (1865 \pm 100)${CsPhPAT}/$K_0$; $R^2 = 0.933$).
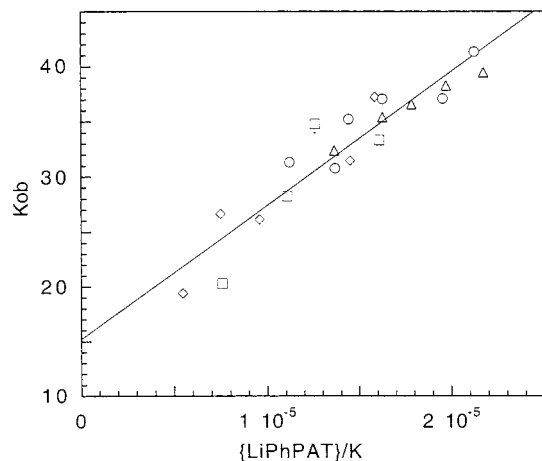

Figure 6. Plot of four runs of K_{ob} vs {LiPhPAT (**1-Li**)}/K_{ob} with DPI as indicator. The equation of the line shown is $(15.21 \pm 1.64) + (1.217 \pm 0.11) \times 10^6$ {LiPhPAT}/K_{ob} and gives $K_{1,2} = 2637$ M^{-1}.

Table 1. Comparison of Properties of Related Enolates

	cesium		lithium	
enolate	pK_0	$K_{1,2}$ M^{-1}	pK_0	$K_{1,2}$ M^{-1}
1-M (MPhPAT)	17.80	1810	11.14	2650
2-M (MPhAT)				1930
4-M (MBPCH)[a]	19.30	1900	12.31	4300
3-M (MPCH)[b]	19.82	1800	12.69	2800
PhCH=C(OM)CH$_2$Ph[c]	18.07	3500	11.62	420
BiPhCH=C(OM)CH$_2$BiPh[d]	17.10	595		
MPhIBP[e]	25.08		15.86	

　[a] References 7 and 15. *[b]* Reference 8. *[c]* Reference 39. *[d]* Reference 13. *[e]* Enolate of *p*-phenylisobutyrophenone; refs 11 and 14.

pK as a function of {CsPhPAT} is shown as the locus of points in Figure 3. Similarly the data for **1-Li** (LiPhPAT) vs DPI are plotted in Figure 6; the results from four separate runs give $pK_0 = 11.14 \pm 0.05$ and $K_{1,2} = 2637 \pm 237$ M^{-1}. This value for $K_{1,2}$ is in good agreement with that derived from SVD. We adopt the average value as $K_{1,2} = 2650$ M^{-1}. The calculated pK as a function of {LiPhPAT} is shown as the locus of points in Figure 4.

　The results are compared in Table 1 with those determined previously for the related conjugated enolates **3-M** (MPCH) and **4-M** (MBPCH). Among the cesium enolates there is a rough trend that more stable enolates (lower pK) have a lower tendency
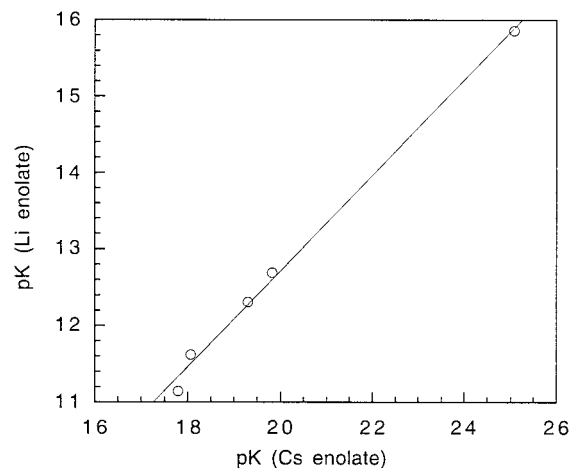
to dimerize, but the trend is clearly affected strongly by other factors. Indeed, for the first three cases the $K_{1,2}$ values are remarkably constant. There is more variation for the lithium enolates, but the total variation in $K_{1,2}$ in this series is only 1 power of ten. The greater tendency of the biphenylyl systems to dimerize compared to phenyl suggests that the *p*-phenyl substituent is freer to rotate in the dimer in which the greater polarization of charge toward the more highly coordinated oxygen requires less charge delocalization; this phenomenon shows up for **1-Li** (LiPhPAT) and **4-Li** (LiBPCH) and is less important, as expected, for the more weakly coordinated cesium enolates. We conclude that within a related set of enolates the aggregation equilibria are similar and affected in a minor way by factors other than basicity. For larger pK differences, however, the trend is clear. For the lithium enolate of *p*-phenyl-sulfonylisobutyrophenone, $pK = 14.69$ and $K_{1,2} = 5.0 \times 10^4$ M^{-1},[10] and the lithium enolate of *p*-phenylisobutyrophenone (LiPhIBP) with $pK = 15.86$ forms a monomer−tetramer equilibrium.[11]

　The lithium enolates have lower pK values than the corresponding cesium enolates. The lithium enolates also have λ_{max} at shorter wavelengths than the cesium analogues, indicating that both are CIP; thus, the shorter O$^-$ Li$^+$ bond distance means a tighter ion pair with a lower ion pair dissociation constant, K_d. By comparison with K_d's for SSIP indicators, the pK difference for MPhPAT of 6.66 units allows an estimate of K_d for LiPhPAT of about 2×10^{-12} M.[23] The point is also shown by a plot of pK(Li) vs pK(Cs) for the enolate data in Table 1. The data give a linear correlation (Figure 7) with a slope of 0.63. For the simplest point charge electrostatic model, this slope would be comparable to the ratio of the O$^-$M$^+$ bond distances. Reasonable distances are 1.6 Å for O−Li and 2.7 Å for O−Cs for a ratio of 0.59.

　Kinetic Study. Kinetic measurements were made by addition of a constant excess amount of alkylating agent (pseudo-first-order conditions) to varying known amounts of enolate and then following the initial rate of reaction of the enolate (10−20%). Kinetics experiments were run with **1-Cs** (CsPhPAT) using *n*-hexyl bromide (HexBr), *n*-hexyl iodide (HexI), methyl tosylate, and methyl brosylate and with **1-Li** (LiPhPAT) using benzyl bromide (BnBr) and *o*-methyl- (*o*-MeBnBr), *o*-chloro-(*o*-ClBnBr), and *m*-chlorobenzyl bromides (*m*-ClBnBr). These compounds were chosen for their low volatility in glovebox handling, HexI was included to test for reaction by SET (single electron transfer), and the lithium enolate required the more reactive benzyl bromides for convenient reaction times.
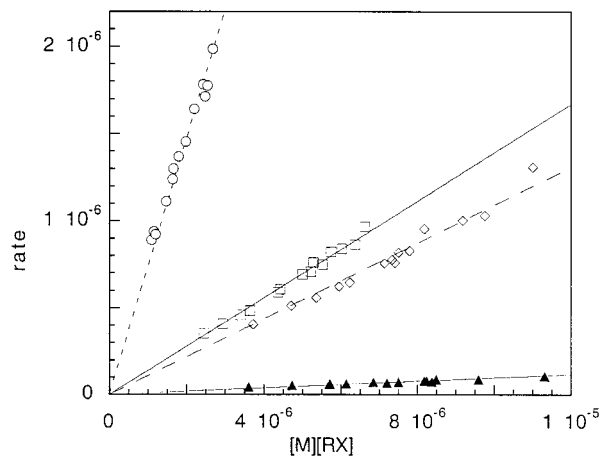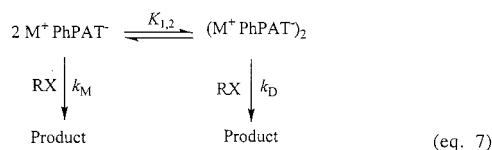

Figure 7. Correlation of pK(Li) with pK(Cs) for the enolate data in Table 1. The line shown is $0.20 + 0.626$ pK(Cs enolate); $R^2 = 0.996$.

10758 *J. Am. Chem. Soc., Vol. 122, No. 44, 2000*

Wang et al.

Figure 8. Plots of rate versus [M][RX] for the reaction of **1-Cs** (CsPhPAT) with alkylating reagents. Slopes of lines shown are triangles, HexBr, 0.0098 ± 0.0002; squares, HexI, 0.139 ± 0.001; diamonds, MeOTs, 0.109 ± 0.002; circles, MeOBs, 0.738 ± 0.009.

In previous studies we showed how the total reaction in eq 7 can be dissected into contributions by monomer and dimer.[10,27] The total rate equation, eq 8, in which M and D refer to monomer and dimer, respectively, can be rearranged to eq 9. Kinetics data plotted as eq 9 would give linear plots in which the slope gives k_M and the intercept is k_D. Several previous examples of such plots gave intercepts indistinguishable from zero, indicating reaction under these conditions solely with the monomer.[7,11,15] This result is also true in the present cases. Figures S17−S19 (Supporting Information) show intercepts indistinguishable from zero.

$$2\ M^+PhPAT^- \underset{}{\overset{K_{1,2}}{\rightleftarrows}} (M^+PhPAT^-)_2$$

$$RX \Big\downarrow k_M \qquad\qquad RX \Big\downarrow k_D$$

$$Product \qquad\qquad\qquad Product \qquad\qquad\qquad (eq.\ 7)$$

$$-d\{MPhPAT\}/dt = k_M[M][RX] + k_D[D][RX] \qquad (eq.\ 8)$$

$$\frac{-d\{MPhPAT\}/dt}{[D][RX]} = k_M \frac{[M]}{[D]} + k_D \qquad\qquad (eq.\ 9)$$

Alternatively, since reaction is primarily with monomer, a plot of rate vs [RX][M] gives directly the second-order rate constant k_M (eq 10).

$$-d\{MPhPAT\}/dt = k_M[RX][M] \qquad (10)$$

The resulting plots are shown in Figures 8 (CsPhPAT), 9 (LiPhPAT), and 10 (LiPhAT), and the rate constants are summarized in Table 2.

The results lead to some interesting conclusions. The reactivity of **2-Li** (LiPhAT) monomer and **1-Li** (LiPhPAT) monomer toward benzyl bromide is the same within experimental error. Little difference would be expected for the effect of a *p*-phenyl group, and the result adds confidence to the overall approach. The reaction of *n*-hexyl iodide with **1-Cs** (CsPhPAT) is 14 times that of the bromide and only slightly more reactive than methyl tosylate. These reactivities are not out of line with typical S_N2 reactions[28] and indicate that the alkyl iodide reaction is not single electron transfer (SET). Reactions with methyl tosylate are now

(27) Abu-Hasanayn, F.; Streitwieser, A. *J. Am. Chem. Soc.* **1996**, *118*, 8136−7.
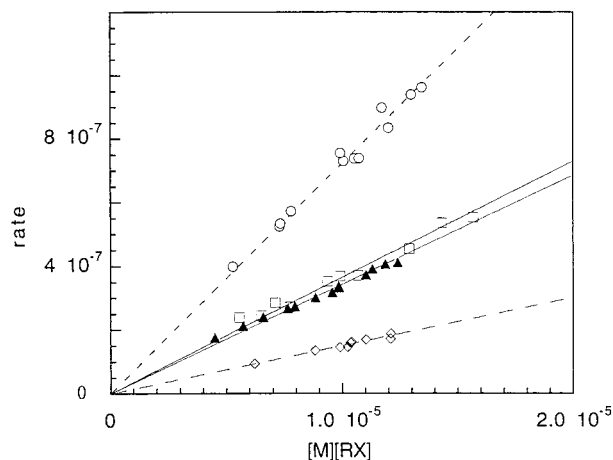(28) Streitwieser, A. *Chem. Rev.* **1956**, *56*, 571.

Figure 9. Plots of rate versus [M][RX] for the reactions of **1-Li** (LiPhPAT) with benzyl bromides. Slopes of lines shown are triangles, BnBr, 0.0343 ± 0.0003; squares, *o*-MeBnBr, 0.0365 ± 0.0006; diamonds, *o*-ClBnBr, 0.0150 ± 0.0002; circles, *m*-ClBnBr, 0.0723 ± 0.0007.
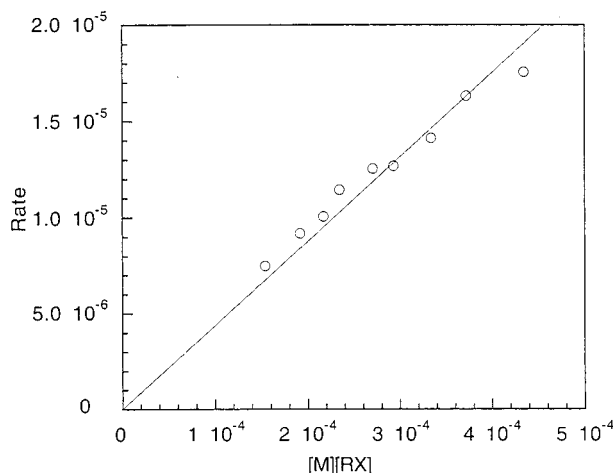

Figure 10. Rate vs [M][RX] for reaction of **2-Li** (LiPhAT) with benzyl bromide. Slope of line shown is 0.036 ± 0.002.

**Table 2.** Second-Order Rate Constants for Reaction of Enolate Monomers with Alkylating Agents in THF at 25 °C

enolate	RX	k_2, M^{-1} s^{-1}	C-/O-alkylation ratio
1-Cs (CsPhPAT)	HexBr	0.0098 ± 0.0002[d]	100% C
	HexI	0.139 ± 0.001[d]	100% C
	MeOTs	0.109 ± 0.002[d]	1/2
	MeOBs	0.738 ± 0.009	1/3
1-Li (LiPhPAT)	BnBr	0.0343 ± 0.0003	100% C
	o-MeBnBr	0.0365 ± 0.0006	
	o-ClBnBr	0.0150 ± 0.0002	100% C
	m-ClBnBr	0.0723 ± 0.0007	
2-Li (LiPhAT)	BnBr	0.036 ± 0.002	100% C

available for three cesium enolate monomers. These reactivities are summarized in Table 3. Comparison of log *k* with the corresponding p*K* values gives a linear correlation with a Brønsted slope of 0.28 (Figure S20, Supporting Information); that is, the basicity of the cesium enolates is a valid measure of ion pair nucleophilicity. The situation is entirely different for lithium enolates. As summarized in Table 3 data are available for the reactivities of four lithium enolate monomers with *m*-chlorobenzyl bromide, and these show no correlation at all with p*K*. For the tighter lithium enolate ion pairs, increasing nucleophilicity accompanying greater basicity is balanced

Table 3. Second-Order Rate Constants of Alkylating Agents with Different Enolate Monomers in THF at 25 °C

enolate	k_2 with MeOTs, $M^{-1} s^{-1}$	k_2 with *m*-ClBnBr, $M^{-1} s^{-1}$
CsPhIBP[a]	14.5	
4-Cs (CsBPCH)[b]	0.46	
1-Cs (CsPhPAT)	0.109	
LiPhIBP[c]		0.255
3-Li (LiPCH)[d]		1.34
4-Li (LiBPCH)[e]		1.47
1-Li (LiPhPAT)		0.0723

[a] Cesium enolate of *p*-phenylisobutyrophenone, ref 14. *[b]* Reference 15. *[c]* Lithium enolate of *p*-phenylisobutyrophenone, ref 11. *[d]* Reference 8. *[e]* Reference 7.

Scheme 1
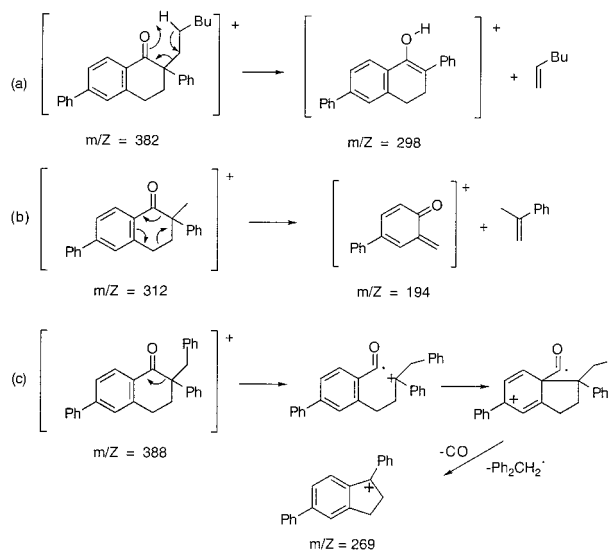
against the greater difficulty in increasing the oxygen−lithium bond distance in going to the transition state and more subtle steric effects at the reacting carbon. This aspect is also brought out by the effect of ortho-substitution with different lithium enolates; for example, the relative rates for the series BnBr, *o*-ClBnBr, *o*-MeBnBr vary by a factor of 2 between reaction with **1-Li** (LiPhPAT) and **4-Li** (LiBPCH),[7] even though both enolates appear to have similar steric environments around the reacting carbon.

Finally, reaction products for several of the reactions were determined by GC-MS. For the reactions for **1-Cs** (CsPhPAT) with hexyl bromide and iodide, only one product was observed; it was readily identified as the C-alkylation product because the base MS peak at $m/z = 298$ (M − C_6H_{12}) is the expected McLafferty rearrangement product (Scheme 1a). The reactions of **1-Cs** (CsPhPAT) with methyl tosylate and brosylate give two products. That coming from the GC first is identified as the O-alkylation product because the base peak is also the parent, $m/z = 312$. The only important fragment peak is $m/z = 221$ (M − PhCH₂) corresponding to deep-seated rearrangement. The second product is identified as the C-alkylation product. The base peak at $m/z = 194$ (M − PhC₃H₅) is rationalized in Scheme 1b. The reactions of **2-Li** (LiPhAT) and **1-Li** (LiPhPAT) with benzyl bromide also give single products identified as those of C-alkylation; the base peaks at $m/z = 193$ and 269, respectively, are rationalized in Scheme 1c. A preparative scale reaction was run with **1-Li** (LiPhPAT) and *o*-chlorobenzyl bromide. The product was identified as the C-alkylation product by NMR; in particular, a signal for the −O−CH₂− group is missing. These results for the C-/O-alkylation ratio are summarized in Table

2. All of the alkyl halides give complete C-alkylation, in agreement with previous results.[7,11,14,15] Only in the case of the most basic enolate, CsPhIBP, does benzyl chloride give a small amount (3%) of O-alkylation.[14] Both LiPhIBP and CsPhIBP give comparable amounts of C- and O-alkylation with methyl sulfonates.[11,14] With either CsBPCH or LiBPCH, methyl sulfonates give only C-alkylation,[7,15] in contrast to the present case of **1-Cs** (CsPhPAT) where mostly O-alkylation was observed. The difference might mean that the enolate carbon in **1** (PhPAT) is more sterically hindered, thus directing more reaction toward oxygen. These generalizations can be added to those summarized by le Noble three decades ago.[29]

Conclusion

The cesium and lithium enolates of **1**, 2,6-diphenyl-α-tetralone, and the lithium enolate of **2**, 2-phenyl-α-tetralone, show monomer−dimer equilibria in dilute THF solution at 25 °C with $K_{1,2} = 10^3 M^{-1}$, the same magnitude found previously for the enolates of another conjugated ketone, **4**, α-biphenylylcyclohexanone. At synthesis concentrations of >0.1 M, these enolates are >90% dimer. As in all of our enolate studies thus far, the dimers are much less reactive in alkylation reactions than the monomers.[30] Monomeric **1-Cs** (CsPhPAT) is less reactive in such alkylations than more basic cesium enolates, but for lithium enolates there appears to be no simple relationship between ion pair basicity and alkylation reactivity. Methyl sulfonates give mostly O-alkylation with **1-Cs** (CsPhPAT), but both enolates give only C-alkylation with alkyl halides. The alkylation with hexyl iodide appears to be a normal ion pair S_N2 reaction and not SET.

Experimental Section

All UV measurements were carried out in a glovebox under an argon atmosphere at a constant temperature of 25.0 ± 0.1 °C, maintained by a cooling bath. The sample compartment located in the floor of the glovebox was connected to a Shimadzu 3801 spectrometer with fiber optic cables. THF was purified as described previously.[31] The alkylating agents and indicators were purified by vacuum sublimation or distillation.

2,6-Diphenyl-1-tetralone, 1. 6-Phenyltetralin[32] was oxidized with chromium trioxide in acetic acid by following the procedure of Allinger and Jones[33] in 57% yield. NMR showed the product to be a mixture of 95% 6-phenyl-α-tetralone and 5% 7-phenyl-α-tetralone (5.3%). Pure 6-phenyl-α-tetralone was obtained by recrystallization twice and sublimation three times, mp 114−115 °C (lit. 105−7 °C,[34] 106−8 °C,[35] 112.5−113.5 °C[36]).

2,6-Diphenyl-α-tetralone, **1**, was prepared by reaction with iodobenzene and potassium *tert*-butoxide in DMSO by following a literature procedure[16] except for the use of argon in place of nitrogen. The product was laboriously separated from unreacted 6-phenyltetralone by differential sublimation under high vacuum to give a 3% yield: mp 149−150 °C; ¹H NMR (300 MHz, CDCl₃) δ 8.18 (d, $J = 8.16$ Hz, 1H), 7.65 (d−t, $J_1 = 6.86$ Hz, $J_2 = 1.53$ Hz, 2H), 7.58 (d−d, $J_1 = 8.18$ Hz, $J_2 = 1.74$ Hz, 1H), 7.51−7.39 (multi, 5H), 7.37−7.34 (multi, 1H), 7.30 (d−t, $J_1 = 7.12$ Hz, $J_2 = 1.46$ Hz, 1H), 7.27−7.17 (multi, 2H), 3.84 (t, $J = 7.94$ Hz, 1H), 2.52−2.44 (multi, 2H), 3.24−3.00 (multi,

(29) le Noble, W. *Synthesis* **1970**, 1−6.
(30) This conclusion contrasts with some others based on product studies of methylation in ethereal solvents: Jackman, L. M.; Lange, B. C. *J. Am. Chem. Soc.* **1981**, *103*, 4494−9.
(31) Gronert, S.; Streitwieser, A., Jr. *J. Am. Chem. Soc.* **1986**, *108*, 7016−22.
(32) Hey, D. H.; Wilkinson, R. *J. Chem. Soc.* **1940**, 1030.
(33) Allinger, N. L.; Jones, E. S. *J. Org. Chem.* **1962**, *27*, 70.
(34) Itoh, K.; Miyake, A.; Tada, N.; Hirata, M.; Oka, Y. *Chem. Pharm. Bull.* **1984**, *32*, 130.
(35) El-Zohry, M. F.; El-Khawaga, A. M. *J. Org. Chem.* **1990**, *55*, 4036.
(36) Lyle, T. A.; Daub, G. H. *J. Org. Chem.* **1979**, *44*, 4933.

2H); ^{13}C NMR (400 MHz, CDCl$_3$) δ 197.9, 144.5, 140.0, 139.7, 128.9, 128.5, 128.4, 128.4, 128.2, 127.3, 127.2, 126.9, 125.6, 54.3, 31.2, 28.9; MS (EI, *m/z*, relative intensity), 300 (M$^+$ + 2, 2.7), 299 (M$^+$ + 1, 21.3), 298 (M$^+$, 86.4), 207 (20.6), 194 (100.0), 166 (20.1), 165 (42.8); HRMS C$_{22}$H$_{18}$O calcd 298.1358, found 298.1358. Anal. Calcd for C$_{22}$H$_{18}$O: C, 88.56; H, 6.08. Found: C, 88.66; H, 6.22.

2-Phenyl-1-tetralone, 2. A solution of *n*-BuLi (10 mL, 2.5 M in hexane) was added to 3 mL of diisopropylamine in THF (20 mL) at −78 C followed by 1.4 g of phenylacetic acid and then 1.6 mL of β-phenylethyl bromide. The mixture was stirred at −78 C for 30 min and was gradually allowed to warm to room temperature. The solution was stirred for an additional 10 h. After pumping off the solvent, 100 mL of water was added to the residual yellow oil. After 2 weeks, yellow crystals formed and the solid (0.6 g) was dried and cyclized by following the procedure of Newman. After recrystallization from ethanol and sublimation, 0.4 g of white solid was obtained: mp 73−74 °C (lit.[37,38] 76−77 °C); ^{1}H NMR δ (300 MHz) 8.1 (1 H, d), 7.5 (1 H), 7.4−7.2 (7 H), 3.8 (1 H), 3.1 (2 H), 2.45 (2 H); *m/z* 222.

Kinetic Studies. The enolate solutions were prepared as in the spectral studies, and known amounts of the alkyl halide or sulfonate were added. Excess alkylating agent was used to give pseudo-first-order conditions. The resulting kinetic solutions generally contained 0.0002−0.001 M enolate and 0.006−0.04 M alkylating agent. The enolate absorption was followed for 10−20% of the reaction, and the resulting linear relation with time was used as the initial rate of reaction. The kinetic results are shown graphically in the Supporting Information, and the rate constants are summarized in Tables 2 and 3.

Product Analyses. The reaction mixtures were allowed to run to completion in the glovebox and analyzed by GC-MS (MS given as *m/z*, relative intensity).

(1) 1-Cs (CsPhPAT) + MeOTs: both C- and O-products, C/O = 1.0/2.0. 2-MePhPAT (C-alkylation), 314 (M + 2, 0.9), 313 (M + 1, 6.3), 312 (M, 25.2), 207 (10.4), 195 (15.3), 194 (100.0), 165 (53.2). O-MePhPAT (O-alkylation), 314 (M + 2, 3.3), 313 (M + 1, 26.3), 312 (M, 100.0), 310 (2.4), 297 (3.7), 296 (4.7), 281 (8.5), 269 (11.8), 235 (5.7), 222 (8.2), 221 (45.9).

(2) 1-Cs (CsPhPAT) + MeOBs: both C- and O-products, C/O = 1.0/3.2).

---

(37) Newman, M. S. *J. Am. Chem. Soc.* **1938**, *60*, 2847.

(38) Newman, M. S. *J. Am. Chem. Soc.* **1940**, *62*, 870.

(39) Gareyev, R.; Ciula, J. C.; Streitwieser, A. *J. Org. Chem.* **1996**, *61*, 4589−93.

(3) 1-Cs (CsPhPAT) + HexBr or HexI. The solution was taken out of box and carried out on GC-MS directly. Both reactions gave only one product: 384 (M + 2, 3.28), 383 (M + 1, 21.60), 382 (M, 70.17), 367 (0.05), 354 (0.06), 353 (0.11), 311 (0.46), 305 (0.09), 299 (24.38), 298 (100.0), 297 (20.95), 278 (5.01), 269 (16.94), 221 (6.40), 207 (73.18).

(4) 1-Li (LiPhPAT) + BnBr. Only one product was found on GC-MS: 389 (M + 1, 22.0), 388 (M, 89.3), 310 (5.7), 298 (14.7), 297 (68.4), 269 (100.0), 194 (38.0).

(5) 1-Li (LiPhPAT) + 2-ClBnBr. The reaction was carried out on a preparative scale. A vial containing 5.295 mg of LDA and 5.40 g of THF was shaken and 14.7 mg of PhPAT was added. The solution was left in the glovebox for 2 days to complete the formation of LiPhPAT. Then 21.0 μL of 2-ClBnBr was added and the solution was mixed. After 1 week in the glovebox the solution was quenched with 1 drop of water. GC-MS showed only one product identified as that of C-alkylation. Solvent was removed, and the residue was purified on preparative TLC to give 21.0 mg of product; MS (*m/z*, relative intensity), 424 (M + 2, 0.65), 423 (M + 1, 0.52), 422 (M, 1.80), 389 (5.44), 388 (32.30), 387 (100.0), 386 (3.42), 345 (0.62), 310 (0.56), 309 (0.72), 298 (8.45), 297 (32.73), 296 (6.73), 270 (11.99), 269 (52.19), 194 (22.80); HRMS C$_{29}$H$_{23}$^{35}ClO calcd 422.1437, found 422.1445; C$_{29}$H$_{23}$^{37}ClO calcd 424.1408, found 424.1421; ^{1}H NMR (400 MHz, CDCl$_3$) δ (ppm) 8.26 (d, J = 8.22 Hz, 1H), 7.51 (t−d, J_1 = 6.98 Hz, J_2 = 1.45 Hz, 3H), 7.41 (t−d, J_1 = 7.78 Hz, J_2 = 1.95 Hz, 2H), 7.36− 7.30 (multi, 2H), 7.28−7.22 (multi, 5H), 7.10 (t−d, J_1 = 7.41 Hz, J_2 = 1.67 Hz, 1H), 7.02 (t−d, J_1 = 7.51 Hz, J_2 = 1.27 Hz, 1H), 6.88 (d−d, J_1 = 7.68 Hz, J_2 = 1.66 Hz, 1H), 3.69 (d, J = 13.78 Hz, 1H), 3.44 (d, J = 13.78 Hz, 1H), 2.88 (t−d, J_1 = 17.02 Hz, J_2 = 4.12 Hz, 1H), 2.81−2.75 (multi, 2H), 2.29 (t−d, J_1 = 13.06 Hz, J_2 = 4.89 Hz, 1H); ^{13}C NMR (400 MHz, CDCl$_3$) δ (ppm) 199.1, 145.8, 143.8, 139.9, 138.7, 135.8, 135.7, 133.0, 131.6, 129.3, 128.8, 128.8, 128.5, 128.1, 127.6, 127.4, 127.2, 127.1, 127.0, 126.2, 125.4, 55.9, 41.5, 30.2, 25.8.

Supporting Information Available: Additional tables and figures. This material is available free of charge via the Internet at http://pubs.acs.org.

JA0010002